International Journal of Robotics and Control Systems
Vol. 4, No. 2, 2024, pp. 758-778
ISSN 2775-2658
http://pubs2.ascee.org/index.php/ijrcs

Revolutionizing Anemia Classification with Multilayer Extremely Randomized Tree Learning Machine for Unprecedented Accuracy

Dimas Chaerul Ekty Saputra [a,1,*], Elvaro Islami Muryadi [b,c,2], Irianna Futri [d,3], Thinzar Aung Win [e,4] Khamron Sunat [a,5], Tri Ratnaningsih [f,6]

[a] Department of Computer Science, College of Computing, Khon Kaen University, Khon Kaen 40002, Thailand
[b] Department of Community, Occupational, and Family Medicine, Faculty of Medicine, Khon Kaen University, Khon Kaen 40002, Thailand
[c] Department of Public Health, Faculty of Health Sciences, Adiwangsa Jambi University, Jambi 36138, Indonesia
[d] Department of International Technology and Innovation Management, International College, Khon Kaen University, Khon Kaen 40002, Thailand
[e] Department of Information Technology, Stamford International University, Bangkok 10250, Thailand
[f] Department of Clinical Pathology and Laboratory Medicine, Faculty of Medicine, Public Health and Nursing, Gadjah Mada University, Yogyakarta 55281, Indonesia
[1] dimaschaerulekty.s@kkumail.com; [2] elvaroislamimuryadi.e@kkumail.com; [3] irianna.f@kkumail.com;
[4] thinzaraung.win@stamford.edu; [5] skhamron@kku.ac.th; [6] triratnaningsih@ugm.ac.id
* Corresponding Author

ARTICLE INFO

Article history
Received April 01, 2024
Revised May 01, 2024
Accepted May 24, 2024

Keywords
Multilayer Extremely Randomized Tree Learning Machine;
Anemia;
Deep Learning;
Machine Learning;
Stacking Model

ABSTRACT

Anemia is a prevalent global health issue that is characterized by a deficit in red blood cells or low levels of hemoglobin. This condition is influenced by various causes, including nutritional inadequacies, chronic diseases, and genetic predisposition. The incidence of the phenomenon exhibits variation across different geographical regions and demographic groups. This pioneering research investigates the identification and classification of anemia, potentially leading to transformative advancements in the discipline. The classification of anemia encompasses four distinct groups, namely Beta Thalassemia Trait, Iron Deficiency Anemia, Hemoglobin E, and Combination. This comprehensive categorization offers clinicians a more refined and detailed comprehension of the condition. The integration of deep learning and machine learning in the Multilayer Extremely Randomized Tree Learning Machine (MERTLM) model represents a departure from traditional approaches and a significant advancement in the field of medical categorization accuracy. The MERTLM approach integrates randomized tree with multilayer extreme learning machine (M-ELM) representation learning, hence emphasizing the possibility of interdisciplinary collaboration in the field of diagnostics. In addition to its impact on anemia, artificial intelligence (AI) is playing a significant role in revolutionizing medical diagnosis by emphasizing the integration of innovative methods. This study utilizes the combined capabilities of machine learning and deep learning to improve accuracy. Notably, recent developments have resulted in an exceptional accuracy rate of 99.67%, precision of 99.60%, sensitivity of 99.47%, and an amazing F1-Score of 99.53%. This study represents a significant advancement in the field of anemia research, providing valuable insights that may be applied to intricate medical issues and enhancing the quality of patient care.

1. Introduction

Anemia is a significant public health issue that affects populations worldwide [1]. It not only affects physical health but also impairs cognitive and physical abilities, productivity, and overall quality of life [2]. According to the World Health Organization (WHO), approximately 25% of the global population, equivalent to around 1.62 billion people, experience the effects of anemia [3], [4]. Developing nations, specifically pregnant females, minors, and individuals with chronic ailments, experience an inequitable share of the burden [5], [6]. Accurate categorization of different subtypes of anemia is crucial for the implementation of effective treatment strategies. However, conventional approaches frequently encounter difficulties, resulting in erroneous classifications and substandard healthcare provision [7], [8]. The complex interplay of various causative factors, including malnutrition and genetics, increases the intricacy of classifying anemia, necessitating customized approaches for diagnosis and treatment [9].

Furthermore, the dependence of conventional methods on the manual interpretation of laboratory results, which is susceptible to human error, underscores the need for innovative and automated approaches to ensure precise classification [10]-[16]. In consideration of this matter, a scholarly investigation conducted by [17] shed light on the significance of hemoglobin, a crucial molecule found in red blood cells, in the process of oxygen transportation. Sickle cell disease perturbs the equilibrium, causing a transformation of previously pliable cells into distorted shapes that impede the flow of blood, resulting in a series of health complications [18].

Timely identification is a feasible approach to progress in this circumstance. Timely detection of sickle cell disease enables the creation of personalized treatments; nevertheless, manual assessment is both laborious and susceptible to mistakes [19], [20]. The algorithm for the multilayer perceptron classifier is a revolutionary solution that effectively detects sickle cells using various methods. A differentiation exists among the three categories of erythrocytes, namely normal (N), sickle cell (S), and thalassemia (T) [21], [22]. The fundamental objective of validation is to assess the accuracy of the algorithm. The program engages in competition within the domains of mining and machine learning by leveraging a dataset sourced from the Thalassemia and Sickle Cell Society. The narrative around the interplay between hemoglobin and sickle cell disease is evolving in conjunction with scientific progress. The multilayer perceptron classifier method, under the guidance of data mining experts, enhances the quality of diagnostics and patient care by facilitating speedy and precise identification [23].

The stage undergoes a shift, drawing attention to an exceptional partnership between microfluidic technology and machine learning [24]. This union creates an advanced clinical diagnosis system that deeply comprehends cellular behavior. For rare hereditary hemolytic anemia (RHHA), a microfluidic device mimics the spleen's role in eliminating faulty red blood cells. Video data analysis enhances our grasp of RHHA within this framework. This innovation strives to enhance diagnostics and RBC deformability assessment, achieved through precise 2D alignment and narrow passages, revealing their endurance. Collaboration encompasses the majority voting scheme and maximum sum of scores, skillfully interlacing analysis. At the peak of technology, a robust platform emerges, distinguishing healthy individuals from RHHA patients. The integration of microfluidic precision and machine learning advances clinical diagnostics, enabling intelligent decision-making and comprehensive patient care [25].

Anemia's hidden presence, hindered by invasive methods and financial constraints, finds a solution by merging cutting-edge medical tech with machine learning. The innovation could mitigate anemia risks, altering its trajectory and impact. As machine learning advances, anemia detection could transform, enabling proactive intervention and better patient outcomes [26]. Various other examinations merit consideration, including red blood cell (RBC) assessments, hemoglobin (Hb) measurements, hematocrit (HCT) levels, mean corpuscular volume (MCV) analysis, mean corpuscular hemoglobin (MCH) evaluation, mean corpuscular hemoglobin concentration (MCHC) assessment, and red-cell distribution width (RDW) measurements [27].

This study seeks to employ the Multilayer Extremely Randomized Tree Learning Machine (MERTLM) to tackle the classification of various forms of anemia. This study provides significant contributions in three key aspects:

1. The utilization of the MERTLM approach is proposed in this study to develop a unique classification model that integrates machine learning and deep learning techniques. This model incorporates randomized trees and multilayer extreme learning machines to classify anemia.
2. It is advisable to retain the factors considered throughout the classification process, even if their influence on the dataset is minimal.
3. Presenting various categorization models incorporating many independent factors.

The present paper is structured into five distinct sections. Section 1 serves as an introductory segment that provides an overview of the problem's background, outlines the objectives, and highlights the research contributions. Section 2 encompasses a comprehensive examination of existing literature. Section 3 provides a comprehensive description of the materials and procedures employed in the study. Section 4 provides an account of the research findings and comprehensively analyzes and interprets these results. Section 5 of this study encompasses the conclusions drawn from the findings and provides ideas for future research endeavors.

2. Literature Review

After doing a study using VOSViewers and obtaining article data from SCOPUS, which consisted of 103 publications, it is evident that there is a substantial body of research on the intersection of anemia and machine learning. Furthermore, it is accurate to assert that there exists a substantial amount of study on anemia that utilizes deep learning techniques, however the scope of this research is limited. One plausible hypothesis for the observed phenomena is the ambiguous association between anemia and significant cognitive capacity. Notwithstanding the existence of a conducted study about the pragmatic implementation of artificial intelligence in the management of anemia, the differentiation between these two concepts remains ambiguous. Upon examining the latest journal updates, it is evident that the subject of deep learning has been extensively examined in connection with anemia. Fig. 1 illustrates the advancement of research on anemia, specifically highlighting the use of machine learning, deep learning, and artificial intelligence. However, Fig. 2 displays the patterns of anemia research, categorized by the years of study. The available data indicates that the field of anemia research utilizing artificial intelligence is still in its nascent stages of development.

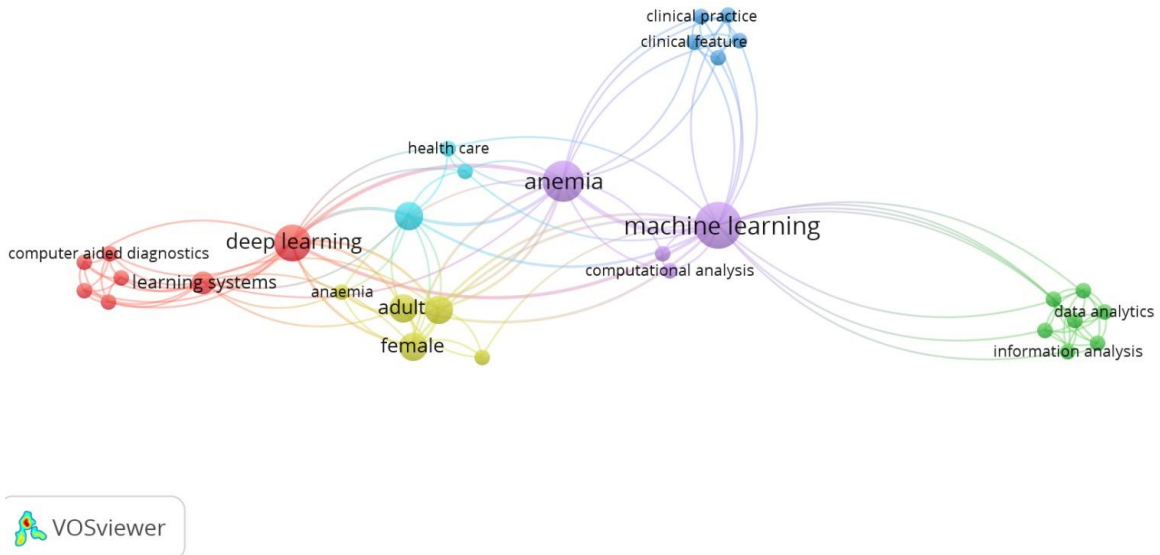

Fig. 1. VOSViewer analysis based on keywords

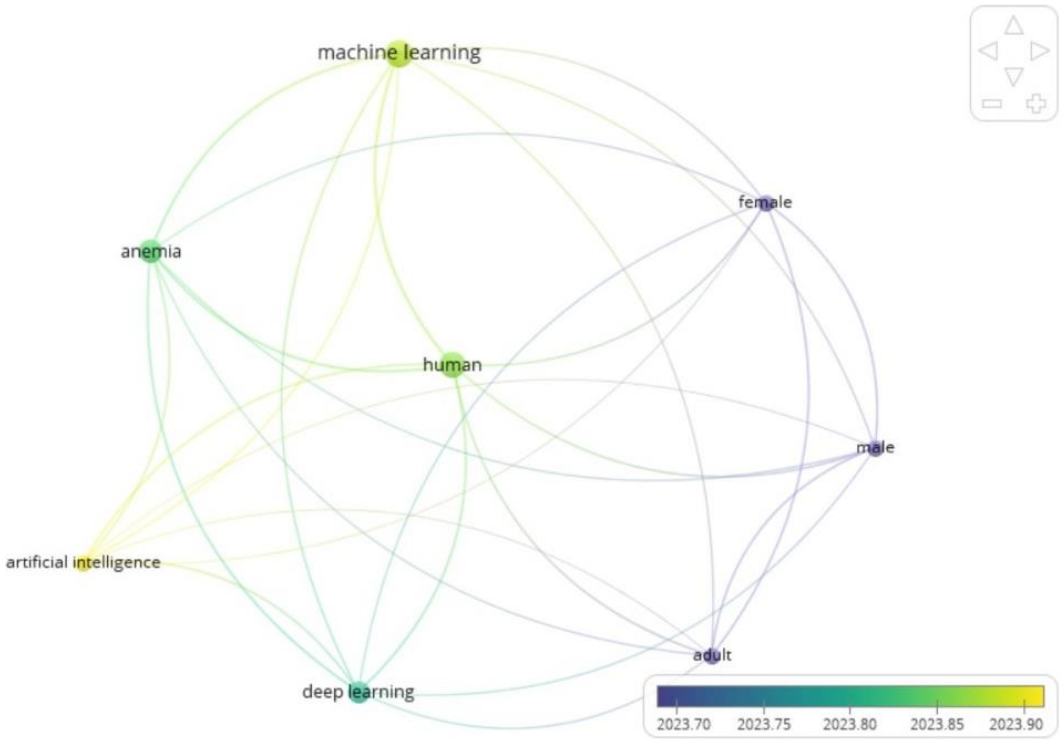

Fig. 2. VOSViewer analysis based on years

Bioinformatics [28] is a rapidly expanding discipline that focuses on predicting clinical outcomes through the use of profiling datasets with numerous variables. Several classification techniques, such as the Random Forest method and protein-protein interaction feature graphs, have been devised by taking into account the functional relationships between features. However, in addition to utilizing gene expression data, these methodologies frequently require external data that may not be provided or may be incomplete. To tackle this particular difficulty, a novel approach is suggested. This approach involves the utilization of a forest-based "feature detector" that incorporates deep neural networks (DNN). The objective of this approach is to develop a classifier that is both resilient and capable of identifying sparse correlations among features inside vast feature spaces.

Although DNN classifiers have demonstrated their efficacy in classification problems, it is a rational decision to construct a supervised feature detector on top of DNN classifiers when the objective is to achieve sparse learning with a decreased parameter count. There are two main reasons why random forests are preferred over alternative models. First and foremost, the Random Forest (RF) model, being an ensemble model, can generate prediction outcomes by aggregating the predictions of its base learners, rather than relying on a single projected probability score. Additionally, the method of assessing the significance of features in each base learner is a basic procedure. In contrast to support vector machines and logistic regressions, this initial element enables the advancement of downstream DNN after the feature detector. This opportunity is not available if the detector produces only a single prediction [28], [29].

The second aspect facilitates feature evaluation for the entire integrated model, in contrast to other classifiers that may not inherently incorporate mechanisms for feature selection. No work has been conducted to date along this path for gene expression data. Nevertheless, the concept of layering classifiers has been implemented and is now widespread in traditional machine learning research.

A study by [30] presented a computational imaging framework that employs a hybrid architecture, integrating deep and ensemble learning techniques. The objective of this framework is to accomplish reliable detection of blood vessels in fundus color images. To identify vessels within the photos, a two-step technique is employed. In the first stage, a deep neural network (DNN) is

utilized to do unsupervised learning to create vessel dictionaries. This approach employs sparsely trained denoising auto-encoders (DAE). Following that, the response of the deep neural network (DNN) is further enhanced through the application of supervised learning techniques, specifically utilizing a random forest algorithm. The success of this approach is demonstrated by its examination using the DRIVE database, where it achieves a maximum average accuracy of 0.9327 and an area under the ROC curve of 0.9195 for vessel detection.

Fundus imaging is extensively utilized as a primary method for the early detection and diagnosis of a range of disorders, including as anemia, diabetic retinopathy, glaucoma, age-related macular degeneration, hypertension, and stroke-induced changes [31]-[36]. The utilization of retinal image analysis has made a substantial impact in reducing the inconsistency in reporting across several observers and even within the same observer, owing to developments in imaging technology. These technological improvements have played a crucial role in mitigating such variability. The primary objective of the suggested methodology is to address the problem of bias in feature representation caused by subjectivity, which has a detrimental impact on the effectiveness of tissue characterization (TC) techniques. The method achieves this by employing unsupervised learning techniques to delineate regions of vessels and nonvascular tissues using available data, and by investigating representations that are particular to the tissue of interest for tumor classification [37]. The present study provides a full description of the hybrid deep neural network-random forest (DNN-RF) architecture employed for vessel detection, along with a concise overview of the research outcomes. Despite being slightly less advanced than the current state-of-the-art approaches that utilize heuristic features, this method demonstrates consistent performance and the capability to identify both general and detailed structures. As a result, it presents a viable solution for addressing the constraints associated with heuristic-dependent and data-driven methods in the analysis of medical images [26], [30].

Cancer is a multifaceted ailment characterized by the aberrant proliferation of cells, their infiltration into surrounding tissues, and their dissemination through the bloodstream and other bodily tissues in human beings [38]. Understanding the genetic components of cancer is crucial in order to achieve precise diagnosis and efficacious treatment. In the field of cancer research, next-generation sequencing techniques have been utilized to examine various genetic alterations in cancer genomes. Extensive investigations into the genomes of cancer have revealed that the genetic changes frequently exhibit variations contingent upon the specific form of cancer. The study conducted by Lawrence et al. revealed that there is significant variation in the mutations discovered in genes relevant to different types of cancer. This finding underscores the distinctiveness of mutations observed in various categories of cancer [39].

A study by [40] confirms that the key criteria used to classify different forms of cancer are mostly based on the distinct genetic features exhibited by the respective tissues under investigation. Furthermore, variations in somatic copy numbers and mutation patterns exhibit discernible patterns depending on the specific tissue type. To tackle these issues, this study introduces a novel cancer classification approach known as the Cancer Predictor utilizing an Ensemble Model (CPEM). The construction of CPEM involves the integration of sophisticated machine learning algorithms with a diverse range of somatic abnormalities observed in different types of malignancies, together with the corresponding attributes that these modifications produce. The study authors performed a thorough examination of gene-level mutation profiles, mutation rates, mutation patterns, signatures, and gene-level copy number alterations to evaluate their influence on the accuracy of the classifier. Moreover, the research conducted a more comprehensive investigation of the efficacy of advanced machine learning classifiers in the context of feature selection and cancer classification.

The approach being suggested represents the most precise technique currently available for the classification of various types of cancer. It encompasses the whole range of cancer types documented in the TCGA database. The present study evaluated the efficacy of four frequently employed machine learning classifiers, namely random forests, one-vs-rest support vector machines (SVM), k-nearest neighbors (KNN), and fully connected deep neural networks (DNN). The objective was to identify

the most optimal classifiers for integration into an ensemble model. Furthermore, the researchers undertook a comprehensive examination of the associations between the outcomes produced by these classifiers. In the realm of cancer research, the widespread availability of DNA sequencing tools has led to significant progress in the quick capture of comprehensive genomic data. However, the escalating magnitude and intricacy of this data present noteworthy obstacles for classification endeavors. This study examines the impact of different input variables, including mutation profiles, mutation rates, mutation patterns and signatures, and somatic copy number variations, on the accurate classification of cancer types [40].

3. Method

3.1. Data Collection

During this study, a comprehensive examination was conducted on 423 individuals who had been diagnosed with various types of anemia and were in the Special Region of Yogyakarta, Indonesia. Data pertaining to anemia were collected over three years, beginning in 2021 and ending in 2023. The procedure of data collection was carried out through a cooperative effort between the Department of Clinical Pathology and Laboratory Medicine at the Faculty of Medicine, Public Health, and Nursing of Universitas Gadjah Mada and the Clinical Pathology Laboratory at Dr. Sardjito Hospital in Yogyakarta, Indonesia. The major purpose of this research was to investigate the hematological characteristics of individuals who have been identified as having either Beta-Thalassemia Trait (BTT), Iron Deficiency Anemia (IDA), Hemoglobin E (HbE), or a combination of two kinds of disease (BTT and IDA or HbE and IDA). A stringent adherence to ethical procedures was maintained throughout the investigation. This was done following the guidelines that were established by the Medical and Health Research Ethics Committee (MHREC) of the Faculty of Medicine, Public Health, and Nursing at Gadjah Mada University - Dr. Sardjito Central General Hospital. A one-of-a-kind reference number, KE/FK/0376/EC/2023, was designed specifically for the investigation. In the period before this one, the reference number that was utilized was KE/FK/1255/EC/2021. The information that was gathered from the 423 patients was instantly entered into a model that was already in place and utilized MERTLM, which resulted in accuracy in the categorization outcomes. The parameters and profiles of the research data are presented in Table 1, which exhibits the laboratory examination profiles.

Table 1. List of laboratory examination parameters and profiles of research data

Parameter	Abbreviation	Unit	Data Profile			
			Minimum	Maximum	Average	Standard deviation
Red Blood Cell	RBC	million /mcL	2.7	7.1	5.1	0.6
Hemoglobin	Hb	g/dL	6.3	17.6	13.2	1.7
Hematocrit	HCT	%	20.1	52.6	40.1	4.5
Mean Corpuscular Volume	MCV	fl	54.6	95.2	79.7	8.5
Mean Corpuscular Hemoglobin	MCH	pg/cell	16.7	34.0	26.2	3.3
Mean Corpuscular Hemoglobin Concentration	MCHC	g/dL	28.0	90.0	33.0	2.8
Red-Cell Distribution Width	RDW	%	11.4	27.9	15.1	2.0

3.2. Research Flow

The laboratory's hematology analyzer generates seven primary characteristics from the data acquired from a comprehensive blood test. The data that has been obtained must be tested further using serum ferritin to get the gold standard from IDA and Hemoglobin Electrophoresis to obtain the gold standard from BTT and HbE. Based on Fig. 3, the amount of data processed for further testing

will be entered into the database. In the database, there will be seven features that are processed. Data labeling is carried out by doctors who are specialists in clinical pathology. After the data enters the database, then the data will be pre-processed. Initial processing includes data cleaning, deletion, MinMax Scaler, and LabelEncoder. Upon completion of the preliminary processing stage, the data will be partitioned into two distinct subsets: 80% of the data will be allocated for training purposes, while the remaining 20% will be reserved for testing. The training data will conduct training using the MERTLM Algorithm. The training data that has undergone training is the data that will become the benchmark for the test data to get a class. The doctor's role here is to provide courses on training data on the results of testing in the laboratory. Test data that has got a class using the MERTLM Algorithm, then the performance testing of the MERTLM algorithm is carried out. After getting the performance results, the results will be reviewed again by the doctor as transparent accountability for the model results and classification results by a doctor specializing in clinical pathology.

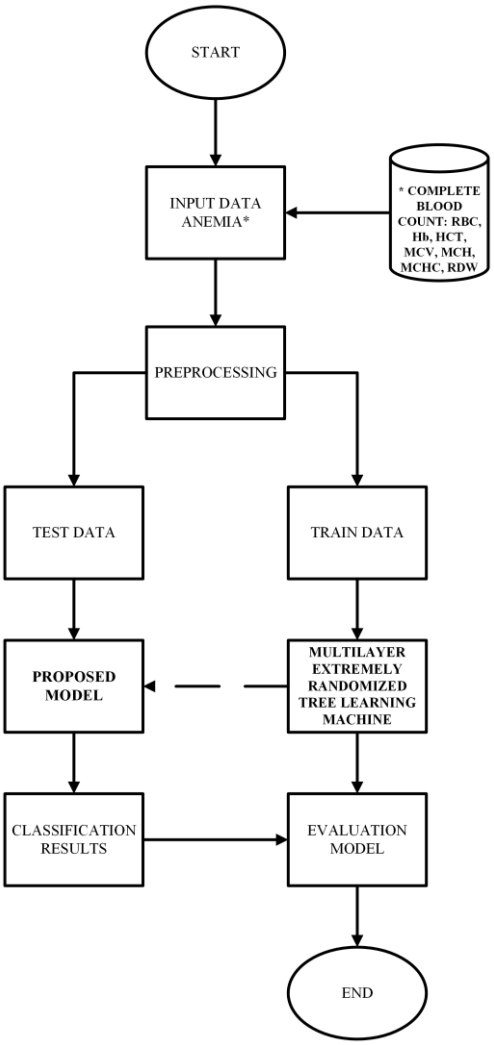

Fig. 3. Research flowchart

3.3. Proposed Model: Multilayer Extremely Randomized Tree Learning Machine

The MERTLM model consists of two distinct components. Using the Stacking technique between Machine Learning, namely Randomized Tree, and Deep Learning, namely extreme learning machine (ELM), this method is proposed. Regular ELM employs a single hidden layer feedforward neural networks (SLFNs) rather than multiple hidden layers [41]-[43]. In this study, however, it was transformed into a Multilayer hidden layer feedforward neural network, subsequently dubbed the multilayer extreme learning machine (M-ELM) [44], [45].

While the forest section of the randomized tree serves as the initial classifier to identify the pattern representation of the raw input data by observing the training results, the M-ELM section serves as the learner to predict the results by employing the newly discovered result representation by the randomized tree. This responsibility is carried out by the network as a whole. These two components are essential to the model's overall functionality [46].

During the forest phase, separate decision trees are generated, transforming the forest into a random forest of trees. Therefore, the random tree model is a natural choice for generating forests. In addition, a variety of forest architectures are conceivable. For instance, if the feature space is sorted and known, one can employ network-guided forests or rapidly generate forests by aggregating trees. Both options are accessible if the feature space is known.

The only form of outcome detector utilized in this investigation is the randomized tree. The MERTLM classifier training consists of two segments. In the first phase, labeled training data is used to match the forest, and in the second step, predictions from each tree are used to train the fully connected M-ELM [46], [47]. Forests are matched against labeled training data in the initial stage [28]. The first stage involves matching forests with the aid of labeled training data. After undergoing a two-stage training procedure, the forest is implemented, and when given the test sample, M-ELM will provide test predictions using the test sample for the entire model.

The MERTLM model views forest F as a collection of randomized trees adapted from [28] organized in the following manner:

$$F(\theta) = \{J_m(\theta_m)\}, \qquad m = 1,2,3,\dots,M, \tag{1}$$

where M is the total number of trees in the forest, $\theta = \{\theta_1, \theta_2, \theta_3, \dots, \theta_M\}$ reflects the parameters inside F within random forest, θ involves dividing variables and their corresponding values. While identifying characteristics, M conforms to the training data X and y, where $X \in R^{n \times p}$, n samples and p characteristics comprise the input data matrix. $y \in R^n$ is the result vector containing the label for categorization. Through the appropriate woodland for observation x_i, In Equation (1), we extract the forecast from each tree in F, then

$$f(x_i; \theta) = (T_1(x_i; \theta_1), \dots, T_M(x_i; \theta_M))^T, \tag{2}$$

where $T_M(x_i; \theta_M) = \hat{y}_{iM}$ the binary forecast of observation x_i supplied by J_m. f_i is a binary vector that summarizes the forest signal and subsequently acts as the ELM's new input characteristics. o_k is the result obtained by Equation (3).

$$o_k = \sum_{j=1}^{N} \beta_j g\left(\sum_{j=1}^{N} w_j x_i + b_j\right), \qquad i = 1, \dots, n, \tag{3}$$

where the following additional feature representations are supplied by the forest in Equation (2), besides x_i represents ith, $\beta_j = [\beta_{j1}, \beta_{j2}, \dots, \beta_{jm}]^T$ indicates the combined weight of the hidden and output layers, $w_j = [w_{j1}, w_{j2}, \dots, w_{jn}]^T$ reflects the difference in weight between the jth hidden layer and the ith input layer, b_j denotes the jth hidden layer's threshold and $g(.)$ represents the activation function using the sigmoid function. Accordingly, the output matrix of hidden layers H Utilizing the sigmoid function, depicts the activation function. Accordingly, the output matrix of hidden layers H and output-hidden layer weights b for the specified input-output sample pairs is now computed as follows $H\beta = O$. H for the transfer function $g(.)$ as in Equation (3). The $w_j.x_i$ is portion becomes the sum of the components of another.w_j and x_i. The N Equation (3) may be expressed concisely as:

$$H\beta = O, \tag{4}$$

where,

$$H = \begin{bmatrix} g(w_1 x_1 + b_1) & \cdots & g(w_N x_1 + b_N) \\ \vdots & \ddots & \vdots \\ g(w_1 x_n + b_1) & \cdots & g(w_N x_n + b_N) \end{bmatrix}_{n \times N}, \quad (5)$$

$$\beta = \begin{bmatrix} \beta_1^T \\ \vdots \\ \beta_N^T \end{bmatrix}_{N \times m}, \text{ and} \quad (6)$$

$$O = \begin{bmatrix} o_1^T \\ \vdots \\ o_N^T \end{bmatrix}_{N \times m}. \quad (7)$$

The H represents the output matrix of the hidden layer. H^T inverse of H according to the generalized Moore–Penrose formula and t is the target class/data label in Equation (8),

$$\hat{\beta} = H^T t. \quad (8)$$

Furthermore, the output weights are calculated via a mathematical transformation, resulting in a decrease in the amount of time required in the training phase, during which the network's parameters are modified periodically using learning parameters (such as learning rate and iteration). The M-ELM algorithm aims to align the output of the actual hidden layers with the expected hidden layer outputs by incorporating a parameter setting step for the subsequent hidden layer [48]. The M-ELM algorithm presents an improved approach for establishing the mapping between input and output signals, known as the M-ELM. The network architecture of M-ELM has an input layer, multiple hidden layers, and an output layer [49]. Each hidden layer consists of j-th hidden neurons. The activation function for the network is chosen as $g(x)$.

The primary objective of the M-ELM method is to perform weight calculation and updating for various layers, including the first hidden layer, the second hidden layer, and each subsequent hidden layer. Additionally, the algorithm also addresses the bias of the hidden layer and the output weights connecting the second hidden layer to the output layer. The workflow of the M-ELM architecture is illustrated in Fig. 2.

Let us consider the training sample datasets x_i, where the matrix H represents the input samples and t represents the labeled samples. The M-ELM algorithm initially consolidates the 15 hidden layers into a single hidden layer. Consequently, the output of the hidden layer may be mathematically represented as $H = g(w_j x_i + b_j)$, where H denotes the hidden layer output, w_j represents the weight parameters on a hidden layer, x_i signifies the input layer and b_j denotes the bias parameters of the first hidden layer. These weight and bias parameters are randomly initialized. Subsequently, the weight matrix β connecting each hidden layer to the output layer can be derived by employing the Equation (8).

The M-ELM algorithm now disentangles the previously fused hidden layers, resulting in the network having many hidden layers. Based on the depicted workflow in Fig. 2, the subsequent hidden layer's output can be acquired in the following manner:

$$H_1 = g(w_1 H + b_1), \quad (9)$$

where the weight matrix w_1 represents the connections between the first hidden layer and the next hidden layer. The matrix H represents the output of the first hidden layer. b_1 denotes the bias of the next hidden layer, while H_1 represents the expected output of the next hidden layer. However, the anticipated result of the second hidden layer can be acquired through computation:

$$H_1 = \beta^T t, \tag{10}$$

where β^T represent the generalized inverse of the matrix H.

The MERTLM model's architecture is seen in Fig. 4 and for the Pseudo Code from MERTLM model as shown in Table 2.

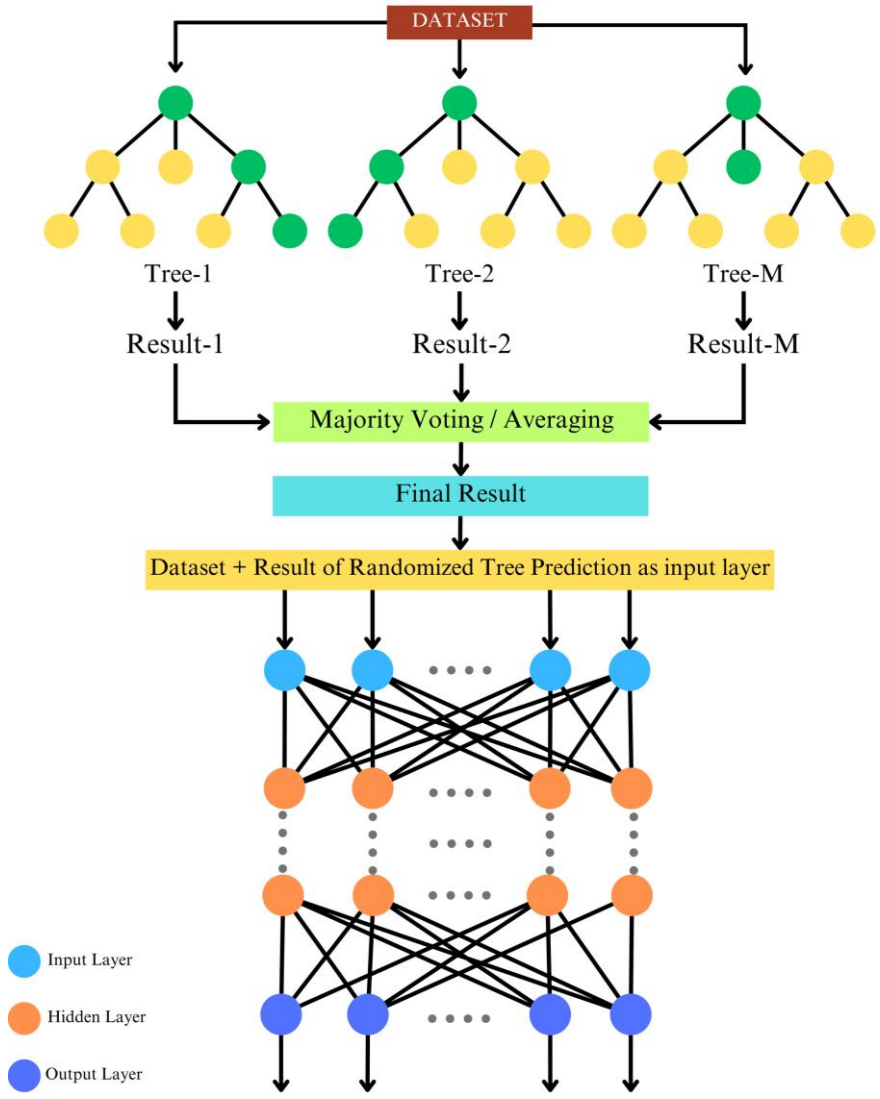

Fig. 4. MERTLM architecture

3.4. Model Evaluation

During the experimental phase, the researcher carefully divided the dataset into two separate segments: the training data and the test data. The aforementioned segments underwent analysis using the Confusion Matrix model, a robust tool utilized to evaluate the precision of classification techniques. In this matrix, a mechanism is employed to measure the efficacy of the classification process, which is a crucial aspect of assessing the model's performance.

The research employed a dataset of four discrete groups, namely Beta Thalassemia Trait, Iron Deficiency Anemia, Hemoglobin E, and Combination. The dataset plays a crucial part in the research. Within the experimental framework, the dataset was efficiently divided into two distinct segments. In this study, a partitioning strategy was employed where 80% of the dataset was allocated for training

purposes, facilitating the acquisition of knowledge by the model. The remaining 20% of the dataset was reserved as test data, serving as a means to assess and validate the performance of the model.

Table 2. Pseudo-code for the MERTLM

Algorithm Multilayer Extremely Randomized Tree Learning Machine

Input:
- training_data: The training dataset with features and corresponding labels
- testing_data: The testing dataset with features (labels are not used in this phase)
- num_trees: The number of trees to create for the Randomized Tree
- num_hidden_layers: The number of hidden layers in the M-ELM
- num_hidden_units: The number of hidden units/neurons in each hidden layer of the M-ELM
- activation_function: The activation function to be used in the hidden layers of the M-ELM using the Sigmoid function

Output: ensemble_model (combined model using stacking).

Begin

```
function MERTLM (training_data, testing_data, num_trees, num_hidden_layers, num_hidden_units, activation_function)
    Step 1: Train the Randomized Tree model
    randomized_tree_model = Randomized_Tree (training_data, num_trees)
    Step 2: Use the Randomized Tree to generate new features for training and
    testing data
    rf_predictions_training =
    random_forest_model.predict(training_data.features)
    augmented_training_data = concatenate(training_data.features,
    rf_predictions_training)
    rf_predictions_testing = random_forest_model.predict(testing_data.features)
    augmented_testing_data = concatenate(testing_data.features,
    rf_predictions_testing)
    Step 3: Train the M-ELM model on the augmented training data
    elm_model = Multilayer_ELM(augmented_training_data,
    num_hidden_layers, num_hidden_units, activation_function)
Step 4: Use the M-ELM to make predictions on the augmented testing data
ensemble_predictions = elm_model.predict(augmented_testing_data)
    return ensemble_predictions
function Randomized_Tree(training_data, num_trees):
    return trained_random_forest_model
function M-ELM(training_data, num_hidden_layers, num_hidden_units, activation_function):
    return trained_elm_model
function concatenate(features, predictions):
    return augmented_data
```

The evaluation of performance in this study entailed the execution of a thorough investigation of a range of classification methods. The present investigation primarily concentrated on the assessment of fundamental metrics, including Accuracy, Precision, Sensitivity, and F1-Score, which hold significant recognition and usage within the respective field. The measures were quantified utilizing Equations (11)-(14) [50]:

$$Accuracy = \frac{TP + TN}{TP + TN + FP + FN} \tag{11}$$

$$Precision = \frac{TP}{TP + FP} \tag{12}$$

$$Sensitivity = \frac{TP}{TP + FN} \tag{13}$$

$$F1 - Score = 2 \times \frac{Recall \times Precision}{Recall + Precision} \tag{14}$$

The entity that is referred to as "TP," which stands for True Positive, is responsible for performing diligent oversight of scenarios in which the system correctly recognizes and classifies positive data. The word "TN," which is a tribute to the idea of True Negative, is used to denote specific negative categorizations. This serves as evidence that the system is able to discern between different types of information. On the other hand, out of nowhere, the letter "FN," which stands for "False Negatives," appears. This is an indication that the system has made the terrible mistake of accidentally identifying negative data. A new component, which is referred to as "FP," which is an abbreviation for "False Positive," is included in addition to the ensemble that was previously discussed. It is the responsibility of this component to draw attention to data that the system, albeit having the best of intentions, incorrectly recognizes as positive. It was determined that the evaluative metrics should be combined and shown in Table 3 of the Confusion Matrix. This effectively illustrated the interaction between the metrics.

Table 3. Confusion matrix [51]

Prediction \ Real Class	True	False
True	TP	FN
False	FP	TN

Within the framework of this complex choreography, the Confusion Matrix assigns specific roles to pivotal terminologies. Equipped with the aforementioned numerical values, the conditions are established for the emergence of Accuracy, Precision, Sensitivity, and F1-Score. This transformation is orchestrated by a symphony of formulas.

The aforementioned formulas effectively capture the fundamental aspects of the Confusion Matrix, encapsulating the performance metrics of the model in a mathematically elegant manner. The F1-Score, within the context of classification, represents a balanced and harmonious measure that encapsulates the intricate interplay between True and False Positives, Negatives, Precision, and Sensitivity.

4. Results and Discussion

The present study employed an experimental analytic approach, applying the suggested MERTLM model, in order to discover and characterize illnesses within a dataset consisting of patients diagnosed with Beta Thalassemia Trait, Iron Deficiency Anemia, Hemoglobin E, and Combination. The model parameters employed in this study are displayed in Table 2. The dataset including instances of anemia patients was utilized and divided into distinct training and testing sets to facilitate the execution of the experimental investigation. The assessment of the classification method in the research entailed employing a Python implementation of the Confusion Matrix. The investigation was conducted using a computing system featuring an Apple M1 processor, 512GB of internal storage, and 8GB of RAM.

The 423 data sets were partitioned into two distinct groups, specifically referred to as the training dataset and the testing dataset. One of the objectives of this study is to propose an alternate framework for addressing the classification of various forms of anemia. The training data was allocated to comprise 80% of the total dataset, while the remaining 20% was designated for testing purposes. The dataset contains a total of seven independent variables.

This study introduces the MERTLM classification model as a proposed method for analyzing the anemia dataset in Table 4. The MERTLM model utilizes a hidden layer implementation comprising a single hidden layer feedforward network (SLFNs) that has been modified by incorporating an MA multilayer feedforward neural network (MFNN). This method can be characterized as a feedforward neural network with one or more hidden layers, in addition to the input and output layers.

The data is conveyed to the input layer, which subsequently undergoes processing through the hidden layer, where a nonlinear activation function is applied. The output of the hidden layer is transmitted to the output layer, which produces the network's output. By employing supervised learning algorithms like backpropagation, the network is able to learn the weights. The algorithm adjusts the weights with the objective of minimizing the discrepancy between the predicted and observed output.

Multilayer feedforward neural networks (MFNNs) have been found to exhibit superior effectiveness compared to single-layer feedforward networks [52], [53]. The primary reason for this phenomenon can be traced to the MFNN's capacity to discern intricate nonlinear connections between input and output data. The applicability of accuracy, precision, sensitivity, and F1-score criteria was assessed for the categorization of the anemia dataset. Table 5 displays the outcomes of the MERTLM model. According to the findings presented in Table 6, the MERTLM model had the highest level of success in classifying the four-class anemia dataset. This achievement was attained by utilizing 80% of the data for training purposes and allocating the remaining 20% for testing. The model exhibited an accuracy rate of 99.67%, precision rate of 99.60%, sensitivity rate of 99.47%, and an F1-Score of 99.53%.

Table 4. MERTLM model

Parameters	Multilayer Extremely Randomized Tree Learning Machine
Target (RMSE)	0.001
Inputs	7
Outputs	4
Hidden layers	15
Training data	453
Testing data	114
Hidden layer neurons	9
Output layer neurons	4
Activation function	Sigmoid

Table 5. Performance results of the MERTLM model

Split Data	Model	Accuracy (%)	Precision (%)	Sensitivity (%)	F1-Score (%)
80% Train – 20% Test	Multilayer Extremely Randomized Tree Learning Machine	99.67	99.60	99.47	99.53

Table 6 presents the normalized confusion matrix of the model utilized in the present study. The matrix is structured such that each column corresponds to a predicted class instance, and each row corresponds to an actual class instance.

To optimize the efficacy of the methodology, the incorporation of MERTLM has been utilized to augment the classification procedure for datasets pertaining to anemia. Hyperparameter tuning is employed to ascertain the ideal number of hidden layers, with an emphasis on increasing the sensitivity score. The analysis determined that the ideal number of nodes for the hidden layer was 15, as evidenced by the data presented in Fig. 5. Table 7 presents the performance index of each class and the proposed strategy, which demonstrates the highest success rate on the anemia dataset. Various machine learning applications utilize the random forest, k-nearest neighbor, support vector machine, extreme learning machine approaches, and multilayer extremely randomized tree learning machine.

The results suggest that the highest level of predictive accuracy was obtained across all categories of anemia.

Table 6. Confusion matrix results from the MERTLM compared to other methods

Model	Classes	BTT	IDA	Hb E	Combination
Random Forest	BTT	18	2	1	0
	IDA	0	26	3	2
	Hb E	2	3	56	0
	Combination	1	0	4	34
K-Nearest Neighbor	BTT	21	0	0	0
	IDA	1	30	0	0
	Hb E	0	0	61	0
	Combination	0	0	1	38
Support Vector Machine	BTT	15	1	5	1
	IDA	2	19	3	1
	Hb E	4	7	48	4
	Combination	0	4	5	33
Extreme Learning Machine	BTT	14	0	0	0
	IDA	0	17	0	0
	Hb E	0	0	50	0
	Combination	0	0	1	32
Multilayer Extremely Randomized Tree Learning Machine	BTT	17	0	0	0
	IDA	0	27	0	0
	Hb E	0	0	61	0
	Combination	0	0	1	46

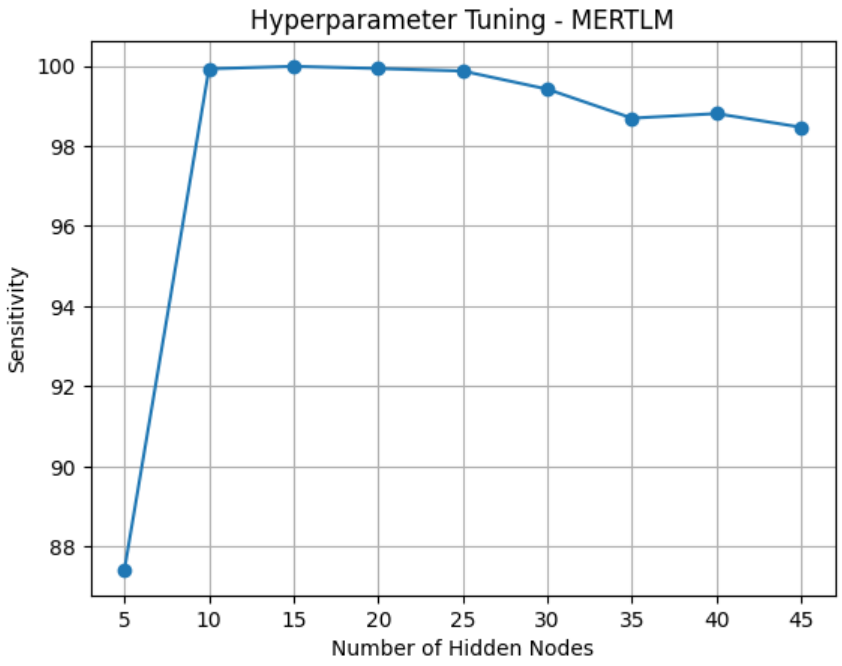

Fig. 5. Hyperparameter tuning hidden layer of MERTLM

Within the field of medicine, the crucial equilibrium between accurately discerning states of health and illness, as well as the potential severe ramifications of incorrect diagnoses, has emphasised the pressing need for dependable diagnostic instruments. The increased utilisation of data mining technologies has been prompted by this phenomenon, in order to guarantee meticulous and reliable evaluations. Given this context, the current study utilised an extreme learning machine (ELM) model to construct a reliable framework for the identification and assessment of anemia. Furthermore, a meticulously designed decision support system was developed to offer invaluable aid to clinicians in their crucial decision-making procedures.

The study utilised a dataset consisting of 339 training samples and 84 test samples. The findings of the research demonstrated that the developed MERTLM approach displayed exceptional performance. In a comparison investigation, it was shown that the MERTLM model outperformed other models, including random forest (RF), k-nearest neighbours (KNN), support vector machine (SVM), and ELM, displaying noteworthy performance metrics. The MERTLM model demonstrated a noteworthy degree of performance, attaining an accuracy rate of 99.67%, a sensitivity rate of 99.47%, a precision rate of 99.60%, and an F1-Score of 99.53%. In stark contrast, the Random Forest (RF) model demonstrated a remarkable accuracy rate of 93.74%, a recall rate of 87.14%, a precision rate of 87.88%, and an F1-Score of 87.46%. In contrast, the KNN model exhibited comparatively lower performance metrics. It achieved an accuracy rate of 99.34%, a recall rate of 98.55%, a precision rate of 98.46%, and an F1-Score of 98.48%. The ELM approach demonstrates an attained accuracy rate of 99.56%, a recall rate of 99.24%, a precision rate of 99.51%, and an F1-Score of 99.37%.

Table 7. Index of performance results for each class in each methods

Model	Classes	Accuracy (%)	Precision (%)	Sensitivity (%)	F1-Score (%)
Random Forest	BTT	95.71	85.71	85.71	85.71
	IDA	93.06	83.87	83.87	83.87
	Hb E	91.16	87.50	91.80	89.60
	Combination	95.04	94.44	87.18	90.67
K-Nearest Neighbor	BTT	99.34	95.45	100	97.67
	IDA	99.34	100	96.77	98.36
	Hb E	99.34	98.39	100	99.19
	Combination	99.34	100	97.44	98.70
Support Vector Machine	BTT	89.84	71.43	68.18	69.77
	IDA	86.47	61.29	76.00	67.86
	Hb E	80.42	78.69	76.19	77.42
	Combination	88.46	84.62	78.57	81.48
Extreme Learning Machine	BTT	100	100	100	100
	IDA	100	100	100	100
	Hb E	99.12	98.04	100	99.01
	Combination	99.12	100	96.97	98.46
Multilayer Extremely Randomized Tree Learning Machine	BTT	100	100	100	100
	IDA	100	100	100	100
	Hb E	99.34	98.39	100	99.19
	Combination	99.34	100	97.87	98.92

Automated detection of blood cell deformities is challenging due to manual errors and time constraints. Artificial neural networks offer a solution. The present study presents a novel methodology, namely the 3-TierDCFNet, which aims to extract morphological characteristics and perform classification of anemia photos, enabling the prediction of disease severity. Module I differentiates between healthy and anemic photos, whilst Module II classifies anemia into moderate or chronic categories. Collaborating with Shaukat Khanum Hospital, new datasets were crafted. Experimental results show the model achieves 91.37% training, 88.85% validation, and 86.06% testing accuracies. F1-Score recall and specificity are also impressive: 98.95%, 98.12%, and 98.12%, respectively [54].

A groundbreaking method, MC-LASSO-ELM, combines Monte Carlo sampling and LASSO for estimating blood hemoglobin levels. It selects samples using random sampling, applies LASSO for variable selection, and merges predictions for the final forecast. When coupled with near-infrared spectroscopy, MC-LASSO-ELM outperforms ELM, MC-ELM, and LASSO-ELM in stability and accuracy. ELM accuracy relies on the activation function and hidden nodes, with the sigmoid function and 66 hidden nodes proving optimal. The ELM sub-model's iteration number (T) significantly impacts computation time and predictive accuracy. (root mean square error of cross-validation (RMSECV) varies substantially and lacks stability with small values. It rapidly declines before 50, then slows beyond 100 [55].

This research expands upon the existing body of knowledge established by previous studies. A study conducted by [56] analyzed a comprehensive dataset consisting of 6,935 instances and 986 variables. The researchers KNN with an accuracy rate of 92.36% and RF with an accuracy rate of 94.16% to classify between BTT and IDA. Another study conducted by researchers Khan et al. (2021) aimed to predict the risk of childhood anemia using various machine-learning techniques, such as KNN and RF. In this study, the RF algorithm demonstrated superior performance compared to the KNN algorithm in terms of accuracy, sensitivity, and specificity. RF achieved an accuracy of 68.50%, the sensitivity of 70.70%, and specificity of 66.40%, surpassing the corresponding values for KNN, which were 61.95%, 65.85%, and 58.20% respectively. Moreover, a study conducted in 2020 demonstrated that RELM achieved a classification accuracy of 95.59% when categorizing 342 patient records into two distinct types of anemia, namely IDA and BTT [41]. Significantly, the extended lymphocyte model also gained prominence during these investigations.

The ELM approach's evolution is evident in the transition from a single hidden layer to the complex structure of a 100-node multilayer hidden layer, giving rise to improved multilayer extreme learning machines (IML-ELM). This novel design employs neural activity during and after training, integrating ortho-normal random connection weights in the initial IML-ELM network. Notably, IML-ELM2, the second iteration, maintains this feature only in its first layer. The strategic evolution significantly reduces computational time. Impressively, the root mean square error test shows promising results of 0.627977, 0.104272 (83%), and 0.092685 (85%), reflecting the notable progress achieved and the effectiveness of the IML-ELM approach in enhancing performance [42].

The series of investigations conducted by researchers [41], [56], [57] enhanced by a diverse range of machine and deep learning methodologies, demonstrates the highest level of achievement in RELM, achieving a notable accuracy of 95.59% in distinguishing between two different types of anemia. Utilizing these foundational elements as building blocks, the implementation of the MERTLM model in the present study presents a promising outlook. The condition known as anemia can be categorized into four distinct subtypes. Recently, there has been a significant improvement in the accuracy of diagnosing anemia, reaching a level of 99.67% accuracy, 99.60% precision, 99.47% sensitivity, and an F1-Score of 99.53%.

Table 8 presents a comparative analysis of the outcomes achieved in previous investigations, focusing on the accuracy parameter. Based on the obtained results, which were effectively achieved using ELM. In contrast to the existing body of research, the study focused on the examination of individuals belonging to four distinct categories, specifically BTT, IDA, HbE, and Combination. The differences made between the four classes were classified to obtain higher accuracy compared to other methods, namely 99.21% for the four classes. In the future, We plan to evaluate the features that are the main factors of anemia patients, so that it can help doctors to speed up diagnosis in every type of anemia that occurs in patients to get a method that will be much more optimal. A deep learning method of classifying anemia data sets and proposing new ones that are suitable for anemia data sets.

5. Conclusion

Discriminating between BTT, IDA, HbE, and their combinations remains a formidable challenge due to the diverse anemia population. The computational model offers a means to expedite anemia screening, resulting in significant time and cost savings. This research further presents a comprehensive analysis of the healthcare system's performance and the challenges encountered in addressing anemia worldwide. It contributes by introducing the MERTLM method, which enhances the efficiency of anemia-type screening. The prediction outcomes are rigorously assessed using a confusion matrix, demonstrating remarkable performance gains. Specifically, the algorithm yielded outstanding results, including a 99.67% accuracy rate, 98.47% sensitivity, 99.60% precision, and an F1-score of 99.53%.

An issue that necessitates particular consideration is the selection of the optimal number of hidden layers to be employed in the MERTLM. The MERTLM technique involves the integration of

two classification algorithms to provide a novel output model. In subsequent studies, we intend to investigate the utilization of an optimization method to ascertain the optimal quantity of hidden layers inside the MERTLM framework, as well as optimizing the MERTLM model itself. The methodology to be investigated is a metaheuristic algorithm method.

Table 8. Competitive results from another method

Authors	Year	Data Size	Number of Classes	Method	Accuracy (%)
Tyas et al. [58]	2020	7,108	9	Multilayer Perceptron	93.77
Çil et al. [41]	2020	342	2	ELM, RELM, SVM, and KNN	95.59
Yıldız et al. [59]	2021	1,663	12	ANN, SVM, Naïve Bayes, and Ensemble Decision Tree	85.60
Wei et al. [60]	2021	428	2	AneNet	98.65
Dejene et al. [61]	2022	11,174	4	Decision Tree, Random Forest, Cat Boost, Extreme Gradient Boost	97.56
Vohra et al. [62]	2022	364	3	Decision Tree, Logistic Regression, MLP, Naïve Bayes, Random Forest, and SVM	96.10
Asare et al. [63]	2023	710	2	CNN, Naïve Bayes, Decision Tree, KNN, and SVM	99.12
Dhalla et al. [64]	2023	324	2	UNet, UNet++, FPN, PSPNet, and LinkNet	94.17
Saputra [50]	2023	190	4	Random Forest, SVM, KNN, and ELM	99.21
Proposed Model	2023	423	4	Random Forest, SVM, KNN, ELM, and MERTLM	99.67

Author Contribution: All authors contributed equally to the main contributor to this paper. All authors read and approved the final paper.

Funding: This research was partial funded by Khon Kaen University Grant for ASEAN Countries and China through the KKU Active Recruitment Project 2022.

Acknowledgment: The research conducted in this study received partial financial assistance from the Khon Kaen University Grant for ASEAN Countries and China through the KKU Active Recruitment Project 2022. Additionally, partial support was provided by the Advance Smart Computing Laboratory, College of Computing, Khon Kaen University. We would like to express our gratitude to PT Abbott and PT Saba Indomedika for their valuable assistance in providing hematological examination reagents. Additionally, we extend our appreciation to CV Dlastika for their support in supplying reagents for hemoglobin analysis. The authors would like to express their gratitude for the support provided by the Artificial Intelligence Center (AIC), College of Computing, Khon Kaen University, Thailand. The endorsement of the final draft of the manuscript for publication.

Conflicts of Interest: The authors declare no conflict of interest.

References

[1] WHO, "Adolescent health epidemiology," *WHO Media Centre*, 2016, https://www.who.int/health-topics/adolescent-health#tab=tab_1.

[2] M. N. Garcia-Casal, O. Dary, M. E. Jefferds, and S. Pasricha, "Diagnosing anemia: Challenges selecting methods, addressing underlying causes, and implementing actions at the public health level," *Annals of the New York Academy of Sciences*, vol. 1524, no. 1, pp. 37-50, 2023, https://doi.org/10.1111/nyas.14996.

[3] E. McLean, M. Cogswell, I. Egli, D. Wojdyla, and B. De Benoist, "Worldwide prevalence of anaemia, WHO Vitamin and Mineral Nutrition Information System, 1993-2005," *Public Health Nutrition*, vol. 12, no. 4, pp. 444–454, 2009, https://doi.org/10.1017/S1368980008002401.

[4] Z. Li *et al*., "Clinical efficacy of myometrial and endometrial microwave ablation in the treatment of patients with adenomyosis who had anemia," *International Journal of Hyperthermia*, vol. 39, no. 1, pp. 1335-1343, 2022, https://doi.org/10.1080/02656736.2022.2131001.

[5] E. A. Costa and J. D. P. Ayres-Silva, "Global profile of anemia during pregnancy versus country income overview: 19 years estimative (2000–2019)," *Annals of Hematology*, vol. 102, pp. 2025-2031, 2023, https://doi.org/10.1007/s00277-023-05279-2.

[6] M. J. Cooper, K. A. Cockell, and M. R. L'Abbé, "The iron status of Canadian adolescents and adults: Current knowledge and practical implications," *Canadian Journal of Dietetic Practice and Research*, vol. 67, no. 3, pp. 130-138, 2006, https://doi.org/10.3148/67.3.2006.130.

[7] M. Manrai, S. Dawra, S. Srivastava, R. Kapoor, and A. Singh, "Anemia in cirrhosis: An underestimated entity," *World Journal of Clinical Cases*, vol. 10, no. 3, pp. 777-789, 2022, http://dx.doi.org/10.12998/wjcc.v10.i3.777.

[8] D. C. E. Saputra, A. Ma'arif, and K. Sunat, "Optimizing Predictive Performance: Hyperparameter Tuning in Stacked Multi-Kernel Support Vector Machine Random Forest Models for Diabetes Identification," *Journal of Robotics and Control*, vol. 4, no. 6, pp. 896-904, 2024, https://doi.org/10.18196/jrc.v4i6.20898.

[9] K. Gemechu, H. Asmerom, L. Gedefaw, M. Arkew, T. Bete, and W. Adissu, "Anemia prevalence and associated factors among school-children of Kersa Woreda in eastern Ethiopia: A cross-sectional study," *PLoS One*, vol. 18, no. 3, p. e0283421, 2023, https://doi.org/10.1371/journal.pone.0283421.

[10] R. T. Sutton, D. Pincock, D. C. Baumgart, D. C. Sadowski, R. N. Fedorak, and K. I. Kroeker, "An overview of clinical decision support systems: benefits, risks, and strategies for success," *NPJ Digital Medicine*, vol. 3, no. 1, p. 17, 2020, https://doi.org/10.1038/s41746-020-0221-y.

[11] V. Baxi, R. Edwards, M. Montalto, and S. Saha, "Digital pathology and artificial intelligence in translational medicine and clinical practice," *Modern Pathology*, vol. 35, no. 1, pp. 23-32, 2022, https://doi.org/10.1038/s41379-021-00919-2.

[12] C. R. Jutzeler *et al*., "Comorbidities, clinical signs and symptoms, laboratory findings, imaging features, treatment strategies, and outcomes in adult and pediatric patients with COVID-19: A systematic review and meta-analysis," *Travel Medicine and Infectious Disease*, vol. 37, p. 101825, 2020, https://doi.org/10.1016/j.tmaid.2020.101825.

[13] A. A. Verma *et al*., "Assessing the quality of clinical and administrative data extracted from hospitals: the General Medicine Inpatient Initiative (GEMINI) experience," *Journal of the American Medical Informatics Association*, vol. 28, no. 3, pp. 578-587, 2021, https://doi.org/10.1093/jamia/ocaa225.

[14] D. B. Olawade, O. J. Wada, A. C. David-Olawade, E. Kunonga, O. Abaire, and J. Ling, "Using artificial intelligence to improve public health: a narrative review," *Front Public Health*, vol. 11, 2023, https://doi.org/10.3389/fpubh.2023.1196397.

[15] S. Preston *et al*., "Toward structuring real-world data: Deep learning for extracting oncology information from clinical text with patient-level supervision," *Patterns*, vol. 4, no. 4, p. 100726, 2023, https://doi.org/10.1016/j.patter.2023.100726.

[16] J. Cadamuro, "Disruption vs. evolution in laboratory medicine. Current challenges and possible strategies, making laboratories and the laboratory specialist profession fit for the future," *Clinical Chemistry and Laboratory Medicine (CCLM)*, vol. 61, no. 4, pp. 558-566, 2023, https://doi.org/10.1515/cclm-2022-0620.

[17] S. Yeruva, M. Sharada Varalakshmi, B. Pavan Gowtham, Y. Hari Chandana, and P. E. S. N. Krishna Prasad, "Identification of sickle cell anemia using deep neural networks," *Emerging Science Journal*, vol. 5, no. 2, pp. 200-210, 2021, https://doi.org/10.28991/esj-2021-01270.

[18] J. S. Gibson and D. C. Rees, "Emerging drug targets for sickle cell disease: shedding light on new knowledge and advances at the molecular level," *Expert Opinion on Therapeutic Targets*, vol. 27, no. 2, pp. 133-149, 2023, https://doi.org/10.1080/14728222.2023.2179484.

[19] A. G. V. Sai and R. Puviarasi, "Diabetes mellitus (DM) detection using SVM algorithm and adaptive neuro fuzzy inference system (ANFIS) for accuracy, specificity, and sensitivity improvement," *AIP Conference Proceedings*, vol. 2816, no. 1, p. 030002, 2024, https://doi.org/10.1063/5.0186149.

[20] A. M. Dayana and W. R. S. Emmanuel, "Deep learning enabled optimized feature selection and classification for grading diabetic retinopathy severity in the fundus image," *Neural Computing and Applications*, vol. 34, no. 21, pp. 18663-18683, 2022, https://doi.org/10.1007/s00521-022-07471-3.

[21] A. R. Belisário *et al*., "Hb S/β-Thalassemia in the REDS-III Brazil Sickle Cell Disease Cohort: Clinical, Laboratory and Molecular Characteristics," *Hemoglobin*, vol. 44, no. 1, pp. 1-9, 2020, https://doi.org/10.1080/03630269.2020.1731530.

[22] S. Pullakhandam and S. McRoy, "Classification and Explanation of Iron Deficiency Anemia from Complete Blood Count Data Using Machine Learning," *BioMedInformatics*, vol. 4, no. 1, pp. 661-672, 2024, https://doi.org/10.3390/biomedinformatics4010036.

[23] P. McCarthy and O. P. Smith, "Hematological problems in pediatric surgery," *Pediatric Surgery*, pp. 119-144, 2023, https://doi.org/10.1007/978-3-030-81488-5_11.

[24] M. Vasina *et al*., "In-depth analysis of biocatalysts by microfluidics: An emerging source of data for machine learning," *Biotechnology Advances*, vol. 66, p. 108171, 2023, https://doi.org/10.1016/j.biotechadv.2023.108171.

[25] V. Rizzuto *et al*., "Combining microfluidics with machine learning algorithms for RBC classification in rare hereditary hemolytic anemia," *Scientific Reports*, vol. 11, no. 1, 2021, https://doi.org/10.1038/s41598-021-92747-2.

[26] A. Mitani *et al*., "Detection of anaemia from retinal fundus images via deep learning," *Nature Biomedical Engineering*, vol. 4, pp. 18-27, 2020, https://doi.org/10.1038/s41551-019-0487-z.

[27] S. S. DeRossi, S. Raghavendra, "Anemia," *Oral Surgery, Oral Medicine, Oral Pathology, Oral Radiology, and Endodontology*, vol. 95, no. 2, pp. 131-141, 2003, https://doi.org/10.1067/moe.2003.13.

[28] Y. Kong and T. Yu, "A Deep Neural Network Model using Random Forest to Extract Feature Representation for Gene Expression Data Classification," *Scientific reports*, vol. 8, no. 1, p. 16477, 2018, https://doi.org/10.1038/s41598-018-34833-6.

[29] A. K. S. Ong *et al*., "Utilization of Random Forest and Deep Learning Neural Network for Predicting Factors Affecting Perceived Usability of a COVID-19 Contact Tracing Mobile Application in Thailand 'ThaiChana," *International Journal of Environmental Research and Public Health*, vol. 19, no. 10, p. 6111, 2022, https://doi.org/10.3390/ijerph19106111.

[30] D. Maji, A. Santara, S. Ghosh, D. Sheet and P. Mitra, "Deep neural network and random forest hybrid architecture for learning to detect retinal vessels in fundus images," *2015 37th Annual International Conference of the IEEE Engineering in Medicine and Biology Society (EMBC)*, pp. 3029-3032, 2015, https://doi.org/10.1109/EMBC.2015.7319030.

[31] K. Callegari et al., "Molecular profiling of the stroke-induced alterations in the cerebral microvasculature reveals promising therapeutic candidates," *Proceedings of the National Academy of Sciences*, vol. 120, no. 16, p. e2205786120, 2023, https://doi.org/10.1073/pnas.2205786120.

[32] D. Nagpal, S. N. Panda and M. Malarvel, "Hypertensive Retinopathy Screening through Fundus Images-A Review," *2021 6th International Conference on Inventive Computation Technologies (ICICT)*, pp. 924-929, 2021, https://doi.org/10.1109/ICICT50816.2021.9358746.

[33] R. Chakraborty and A. Pramanik, "DCNN-based prediction model for detection of age-related macular degeneration from color fundus images," *Medical & Biological Engineering & Computing*, vol. 60, no. 5, pp. 1431-1448, 2022, https://doi.org/10.1007/s11517-022-02542-y.

[34] E. Waisberg, J. Ong, N. Zaman, S. A. Kamran, A. G. Lee, A. Tavakkoli, "A non-invasive approach to monitor anemia during long-duration spaceflight with retinal fundus images and deep learning," *Life sciences in space research*, vol. 33, pp. 69-71, 2022, https://doi.org/10.1016/j.lssr.2022.04.004.

[35] R. Thanki, "A deep neural network and machine learning approach for retinal fundus image classification," *Healthcare Analytics*, vol. 3, p. 100140, 2023, https://doi.org/10.1016/j.health.2023.100140.

[36] K. Shankar, Y. Zhang, Y. Liu, L. Wu and C. -H. Chen, "Hyperparameter Tuning Deep Learning for Diabetic Retinopathy Fundus Image Classification," *IEEE Access*, vol. 8, pp. 118164-118173, 2020, https://doi.org/10.1109/ACCESS.2020.3005152.

[37] D. C. E. Saputra, Y. Maulana, T. A. Win, R. Phann, Wa. Caesarendra, "Implementation of Machine Learning and Deep Learning Models Based on Structural MRI for Identification of Autism Spectrum Disorder," *Jurnal Ilmiah Teknik Elektro Komputer dan Informatika*, vol. 9, no. 2, pp. 307-318, 2023, http://dx.doi.org/10.26555/jiteki.v9i2.26094.

[38] K. Lee, H. oh Jeong, S. Lee, and W. K. Jeong, "CPEM: Accurate cancer type classification based on somatic alterations using an ensemble of a random forest and a deep neural network," *Scientific Reports*, vol. 9, no. 1, p. 16927, 2019, https://doi.org/10.1038/s41598-019-53034-3.

[39] A. Helisa, T. H. Saragih, I. Budiman, F. Indriani, D. Kartini, "Prediction of Post-Operative Survival Expectancy in Thoracic Lung Cancer Surgery Using Extreme Learning Machine and SMOTE," *Jurnal Ilmiah Teknik Elektro Komputer dan Informatika*, vol. 9, no. 2, pp. 239–249, 2023, http://dx.doi.org/10.26555/jiteki.v9i2.25973.

[40] K. A. Hoadley *et al*., "Multiplatform analysis of 12 cancer types reveals molecular classification within and across tissues of origin," *Cell*, vol. 158, no. 4, p. 929-944, 2014, https://doi.org/10.1016/j.cell.2014.06.049.

[41] B. Çil, H. Ayyıldız, and T. Tuncer, "Discrimination of β-thalassemia and iron deficiency anemia through extreme learning machine and regularized extreme learning machine based decision support system," *Medical Hypotheses*, vol. 138, p. 109611, 2020, https://doi.org/10.1016/j.mehy.2020.109611.

[42] G. A. Kale and C. Karakuzu, "Multilayer extreme learning machines and their modeling performance on dynamical systems," *Applied Soft Computing*, vol. 122, p. 108861, 2022, https://doi.org/10.1016/j.asoc.2022.108861.

[43] M. Duan, K. Li, X. Liao and K. Li, "A Parallel Multiclassification Algorithm for Big Data Using an Extreme Learning Machine," *IEEE Transactions on Neural Networks and Learning Systems*, vol. 29, no. 6, pp. 2337-2351, 2018, https://doi.org/10.1109/TNNLS.2017.2654357.

[44] C. J. Zhu, H. D. Yang, Y. J. Fan, B. Fan, and K. K. Xu, "Online spatiotemporal modeling for time-varying distributed parameter systems using Kernel-based Multilayer Extreme Learning Machine," *Nonlinear Dynamics*, vol. 107, pp. 761-780, 2022, https://doi.org/10.1007/s11071-021-06987-y.

[45] Y. Xu, L. Liu, S. Zhang, and W. Xiao, "Multilayer extreme learning machine-based unsupervised deep feature representation for heartbeat classification," *Soft Computing*, vol. 23, pp. 12353–12366, 2023, https://doi.org/10.1007/s00500-023-07861-2.

[46] C. M. Wong, C. M. Vong, P. K. Wong and J. Cao, "Kernel-Based Multilayer Extreme Learning Machines for Representation Learning," *IEEE Transactions on Neural Networks and Learning Systems*, vol. 29, no. 3, pp. 757-762, 2018, https://doi.org/10.1109/TNNLS.2016.2636834.

[47] C. K. L. Lekamalage, K. Song, G. -B. Huang, D. Cui and K. Liang, "Multi layer multi objective extreme learning machine," *2017 IEEE International Conference on Image Processing (ICIP)*, pp. 1297-1301, 2017, https://doi.org/10.1109/ICIP.2017.8296491.

[48] D. Xiao, B. Li, and Y. Mao, "A Multiple Hidden Layers Extreme Learning Machine Method and Its Application," *Mathematical Problems in Engineering*, vol. 2017, 2017, https://doi.org/10.1155/2017/4670187.

[49] J. Tang, C. Deng and G. -B. Huang, "Extreme Learning Machine for Multilayer Perceptron," *IEEE Transactions on Neural Networks and Learning Systems*, vol. 27, no. 4, pp. 809-821, 2016, https://doi.org/10.1109/TNNLS.2015.2424995.

[50] D. C. E. Saputra, K. Sunat, and T. Ratnaningsih, "A New Artificial Intelligence Approach Using Extreme Learning Machine as the Potentially Effective Model to Predict and Analyze the Diagnosis of Anemia," *Healthcare*, vol. 11, no. 5, p. 697, 2023, https://doi.org/10.3390/healthcare11050697.

[51] D. C. E. Saputra, Y. Maulana, E. Faristasari, A. Ma'arif, and I. Suwarno, "Machine Learning Performance Analysis for Classification of Medical Specialties," *Proceeding of the 3rd International Conference on Electronics, Biomedical Engineering, and Health Informatics*, pp. 513-528, 2023, https://doi.org/10.1007/978-981-99-0248-4_34.

[52] Q. Lu, S. Liu, W. Li, and X. Jin, "Combination of thermodynamic knowledge and multilayer feedforward neural networks for accurate prediction of MS temperature in steels," *Material & Design*, vol. 192, p. 108696, 2020, https://doi.org/10.1016/j.matdes.2020.108696.

[53] D. Ersoy and B. Erkmen, "A Stochastic Computing Method For Generating Activation Functions in Multilayer Feedforward Neural Networks," *Electrica*, vol. 21, no. 3, 2021, https://doi.org/10.5152/electr.2021.21043.

[54] M. Shahzad *et al*., "Identification of Anemia and Its Severity Level in a Peripheral Blood Smear Using 3-Tier Deep Neural Network," *Applied Sciences*, vol. 12, no. 10, p. 5030, 2022, https://doi.org/10.3390/app12105030.

[55] K. Wang, X. Bian, M. Zheng, P. Liu, L. Lin, and X. Tan, "Rapid determination of hemoglobin concentration by a novel ensemble extreme learning machine method combined with near-infrared spectroscopy," *Spectrochimica Acta Part A: Molecular and Biomolecular Spectroscopy*, vol. 263, p. 120138, 2021, https://doi.org/10.1016/j.saa.2021.120138.

[56] V. Laengsri, W. Shoombuatong, W. Adirojananon, C. Nantasenamart, V. Prachayasittikul, and P. Nuchnoi, "ThalPred: A web-based prediction tool for discriminating thalassemia trait and iron deficiency anemia," *BMC Medical Informatics and Decision Making*, vol. 19, pp. 1-14, 2019, https://doi.org/10.1186/s12911-019-0929-2.

[57] J. R. Khan, S. Chowdhury, H. Islam, and E. Raheem, "Machine Learning Algorithms To Predict The Childhood Anemia In Bangladesh," *Journal of Data Science*, vol. 17, no. 1, pp. 195–218, 2021, https://doi.org/10.6339/JDS.201901_17(1).0009.

[58] D. A. Tyas, S. Hartati, A. Harjoko and T. Ratnaningsih, "Morphological, Texture, and Color Feature Analysis for Erythrocyte Classification in Thalassemia Cases," *IEEE Access*, vol. 8, pp. 69849-69860, 2020, https://doi.org/10.1109/ACCESS.2020.2983155.

[59] T. Karagül Yıldız, N. Yurtay, and B. Öneç, "Classifying anemia types using artificial learning methods," *Engineering Science and Technology, an International Journal*, vol. 24, no. 1, pp. 50-70, 2021, https://doi.org/10.1016/j.jestch.2020.12.003.

[60] H. Wei, H. Shen, J. Li, R. Zhao, and Z. Chen, "AneNet: A lightweight network for the real-time anemia screening from retinal vessel optical coherence tomography images," *Optics & Laser Technology*, vol. 136, p. 106773, 2021, https://doi.org/10.1016/j.optlastec.2020.106773.

[61] B. E. Dejene, T. M. Abuhay, and D. S. Bogale, "Predicting the level of anemia among Ethiopian pregnant women using homogeneous ensemble machine learning algorithm," *BMC Medical Informatics and Decision Making*, vol. 22, no. 1, p. 247, 2022, https://doi.org/10.1186/s12911-022-01992-6.

[62] R. Vohra, A. Hussain, A. K. Dudyala, J. Pahareeya, and W. Khan, "Multi-class classification algorithms for the diagnosis of anemia in an outpatient clinical setting," *PLoS One*, vol. 17, no. 7, p. e0269685, 2022, https://doi.org/10.1371/journal.pone.0269685.

[63] J. W. Asare, P. Appiahene, E. T. Donkoh, and G. Dimauro, "Iron deficiency anemia detection using machine learning models: A comparative study of fingernails, palm and conjunctiva of the eye images," *Engineering Reports*, vol. 5, no. 11, p. e12667, 2023, https://doi.org/10.1002/eng2.12667.

[64] S. Dhalla *et al*., "Semantic segmentation of palpebral conjunctiva using predefined deep neural architectures for anemia detection," *Procedia Computer Science*, vol. 218, pp. 328-337, 2023, https://doi.org/10.1016/j.procs.2023.01.015.